

DOI: 10.1002/cmdc.201300032

Structure–Activity Relationships of Quinoxaline-Based 5-HT₃A and 5-HT₃AB Receptor-Selective Ligands

Andrew J. Thompson,^[b] Mark H. P. Verheij,^[a] Jacqueline E. van Muijlwijk-Koezen,^[a]
Sarah C. R. Lummis,^{*[b]} Rob Leurs,^[a] and Iwan J. P. de Esch^[a]

Until recently, discriminating between homomeric 5-HT₃A and heteromeric 5-HT₃AB receptors was only possible with ligands that bind in the receptor pore. This study describes the first series of ligands that can discriminate between these receptor types at the level of the orthosteric binding site. During a recent fragment screen, 2-chloro-3-(4-methylpiperazin-1-yl)-quinoxaline (VUF10166) was identified as a ligand that displays an 83-fold difference in [³H]granisetron binding affinity between 5-HT₃A and 5-HT₃AB receptors. Fragment hit exploration, initiated from VUF10166 and 3-(4-methylpiperazin-1-yl)-

quinoxalin-2-ol, resulted in a series of compounds with higher affinity at either 5-HT₃A or 5-HT₃AB receptors. These ligands reveal that a single atom is sufficient to change the selectivity profile of a compound. At the extremes of the new compounds were 2-amino-3-(4-methylpiperazin-1-yl)quinoxaline, which showed 11-fold selectivity for the 5-HT₃A receptor, and 2-(4-methylpiperazin-1-yl)quinoxaline, which showed an 8.3-fold selectivity for the 5-HT₃AB receptor. These compounds represent novel molecular tools for studying 5-HT₃ receptor subtypes and could help elucidate their physiological roles.

Introduction

5-HT₃ receptors are ligand-gated ion channels that are responsible for fast synaptic neurotransmission in the central (CNS) and peripheral nervous systems (PNS). They are involved in physiological functions as diverse as the vomiting reflex, pain processing, reward, cognition, and anxiety, and modulate the release of neurotransmitters such as acetylcholine, cholecystokinin, dopamine, GABA, glutamate, and serotonin itself.^[1] To date, five different subunits (5-HT₃A–5-HT₃E) have been identified, but the homomeric 5-HT₃A- and heteromeric 5-HT₃AB-containing receptors are the most fully characterized.^[1,2] 5-HT₃A receptors are located primarily in the CNS, while 5-HT₃AB receptors may be more abundant in the PNS.^[1,3]

5-HT₃ receptors are members of the Cys-loop family of neurotransmitter-gated receptors that all share a pentameric structure of subunits surrounding a central ion-conducting pore. Each subunit has an extracellular domain, four transmembrane α helices (one of which contributes to the ion conducting pore) and an intracellular domain.^[4] The agonist/competitive antagonist (orthosteric) binding site is located at the interface of two adjacent subunits and is formed by the convergence of

three loops (loops A–C) from the principal (or +) subunit and three β sheets (loops D–E) from the adjacent complementary (or –) subunit.

The two 5-HT₃ receptor subtypes (5-HT₃A and 5-HT₃AB) can be distinguished by differences in their 5-HT concentration–response curves (increased EC₅₀ values and shallower Hill slopes), increased single channel conductance (5-HT₃A = sub-pS; 5-HT₃AB = 16–30 pS), increased rate of desensitization, decreased relative Ca²⁺ permeability, and different current–voltage relationships (5-HT₃A is inwardly rectifying, 5-HT₃AB is linear).^[1b,5] Pharmacologically distinguishing 5-HT₃A from 5-HT₃AB receptors has historically required the use of compounds that bind in the pore, such as bilobalide, ginkgolide, and picrotoxinin.^[6] In contrast, competitive ligands usually have very similar affinities at 5-HT₃A and 5-HT₃AB receptors. Recently, however, a quinoxaline compound (VUF10166) was identified that showed differences in both its binding affinity and functional properties at 5-HT₃A and 5-HT₃AB receptors (Figure 1).^[7] Detailed studies of VUF10166 showed that these differences may stem from a second, allosteric, site only found in the 5-HT₃AB receptor, the occupation of which may increase the rate of ligand dissociation from the adjacent orthosteric site.

The actions of a range of quinoxalines have also been previously studied at both 5-HT₃A and native receptors and re-

[a] Dr. M. H. P. Verheij,⁺ Dr. J. E. van Muijlwijk-Koezen, Prof. R. Leurs, Dr. I. J. P. de Esch
Amsterdam Institute for Molecules Medicines and Systems (AIMMS)
Division of Medicinal Chemistry, Faculty of Sciences
VU University Amsterdam, Amsterdam (The Netherlands)

[b] Dr. A. J. Thompson,⁺ Prof. S. C. R. Lummis
Department of Biochemistry, University of Cambridge, Cambridge (UK)
E-mail: sl120@cam.ac.uk

[⁺] These authors contributed equally to this work.

© 2013 The Authors. Published by Wiley-VCH Verlag GmbH & Co. KGaA. This is an open access article under the terms of the Creative Commons Attribution License, which permits use, distribution and reproduction in any medium, provided the original work is properly cited.

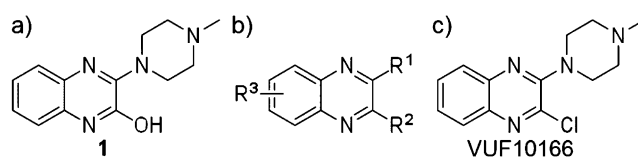


Figure 1. a) Structure of compound 1; b) general structure for all analogues; c) VUF10166.

vealed that these compounds can be relatively potent (sub-micromolar affinities) as antagonists, agonists, and partial agonists, with potential as novel therapeutics.^[6] There is particular interest, for example, in developing quinoxalines which are impermeable to the blood–brain barrier that would target peripheral 5-HT₃ receptors.^[6a] None of these studies, however, have evaluated ligand affinities at specific 5-HT₃ receptor subtypes. In this manuscript, we report the synthesis and binding affinities of a series of quinoxalines and demonstrate subtle differences in structure–activity relationships (SAR) for the 5-HT_{3A} and 5-HT_{3AB} receptor subtypes using competition binding on recombinantly expressed receptors in HEK293 cells.

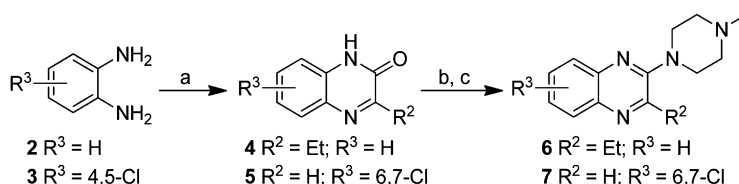
Results and Discussion

Chemistry

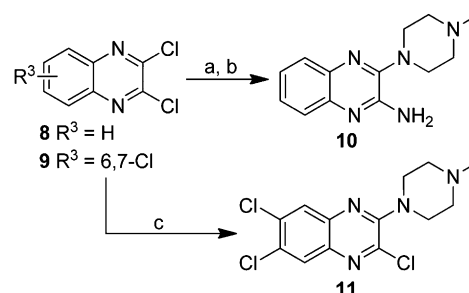
The pharmacophore features of lead compound **1** and VUF10166, and the effects of these features on 5-HT_{3A} and 5-HT_{3AB} receptor affinities, was explored by screening a series of compounds that contain the quinoxaline scaffold (Figure 1 b). Intermediates **4–5** were synthesized via a two-step ring formation between 2-amino aniline **2** or **3** and the appropriate 2-oxo carboxylic acids (Scheme 1). After conversion into the corresponding 2-chloroquinoxalines with phosphorylchloride, subsequent nucleophilic aromatic substitution with *N*-methylpiperazine under microwave conditions gave compounds **6** and **7** in moderate to good yields.

Starting from commercially available chloro-quinoxalines **8** and **9**, different synthetic routes were followed to synthesize compounds **10** and **11** (Scheme 2). Compound **10** was synthesized through two subsequent nucleophilic aromatic substitution reactions. First, the amine moiety was introduced by reacting compound **8** with ammonia in ethanol. Subsequently, the *N*-methylpiperazine group was introduced. Both reactions were performed under microwave conditions. Compound **11** was created in a similar manner, although conventional heating was used for this synthesis.

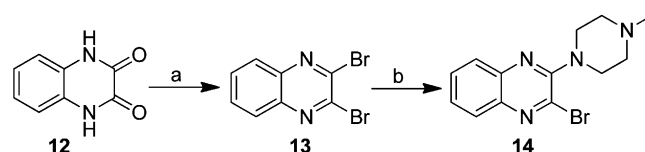
Commercially available quinoxaline-2,3-(1*H*,4*H*)-dione (**12**) was treated with phosphorous pentabromide to form 2,3-dibromoquinoxaline (**13**), which was then allowed to react with *N*-methylpiperazine in toluene at reflux to yield compound **14** (Scheme 3). For compounds **16**, **18**, **19**, and **21**, 2,3-dichloroquinoxaline (**8**) or 2-chloroquinoxaline (**15**) were reacted with the corresponding amines using various solvents and temperatures to yield **16**, **17**, **19**, and **20** in good yields. Boc-protected intermediates **17** and **20** were subsequently deprotected with a 4 M solution of hydrochloric acid in dioxane to give compounds **18** and **21** (Scheme 4). The regioselective synthesis of compound **22** was described earlier by our group.^[9] Here, we used this compound as a precursor in the synthesis of compound **23** (Scheme 5).



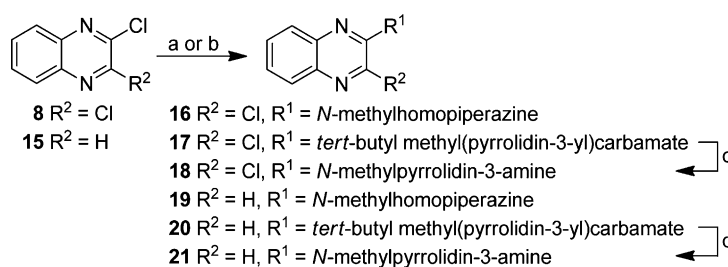
Scheme 1. Synthesis of quinoxalines. Reagents and conditions: a) R₂COCO₂H, CH₃OH, RT, 30 min; b) POCl₃, 100 °C, 1 h; c) *N*-methylpiperazine, mw, 120 °C, or *N*-methylpiperazine, EtOAc, mw, 160 °C, 15 min.



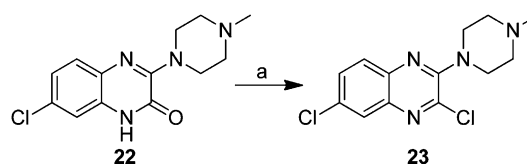
Scheme 2. Synthesis of compounds **10** and **11**. Reagents and conditions: a) 2 M NH₃ in EtOH, in EtOH, 120 °C, 120 min; b) *N*-methylpiperazine, THF, mw, 150 °C, 40 min; c) *N*-methylpiperazine, Et₃N, THF, 80 °C, 96 h.



Scheme 3. Synthesis of 2-bromo-3-(4-methylpiperazin-1-yl)quinoxaline (**14**). Reagents and conditions: a) PBr₅, toluene, 160 °C, 3 h; b) *N*-methylpiperazine, Et₃N, toluene, reflux, 6 h.



Scheme 4. Synthesis of compounds **16**, **18**, **19**, and **21**. Reagents and conditions: a) *N*-methylhomopiperazine, Et₃N, toluene, reflux, overnight; b) *tert*-butyl methyl(pyrrolidin-3-yl)carbamate, K₂CO₃, DMF, 90 °C, 4 h; c) 4 M HCl in dioxane, RT, overnight.



Scheme 5. Synthesis of compound **23**. Reagents and conditions: a) POCl₃, DiPEA, toluene, reflux, 20 h.

Biochemical evaluation and SAR studies

SAR of quinoxaline compounds for the 5-HT_{3A} receptors

Target compounds were evaluated using competition binding with the 5-HT₃-specific ligand [³H]granisetron; the results are summarized in Table 1. SAR data in this table are presented with a focus on different substitution patterns at the R¹, R²,

and R³ positions of the quinoxaline core scaffold. We found that several quinoxaline compounds show clear differences in their binding affinities at the two receptor subtypes, and the subtype preference differs within the series.

First, the SAR of the series will be described for the 5-HT_{3A} receptor subtype. The alcohol moiety at the R² position implies that compound 1 can adopt two different tautomeric states. It

Table 1. Competition binding affinities for quinoxalines at 5-HT_{3A} and 5-HT_{3AB} receptors with respect to substitutions at R¹, R², and R³.

Compd	R ¹	R ²	R ³	5-HT _{3A}		5-HT _{3AB}		Fold diff. ^[a]
				pK _i (A)	n	pK _i (AB)	n	
1		OH	H	8.93 ± 0.21	11	9.36 ± 0.06	11	+2.7
28		OMe	H	9.18 ± 0.16	6	8.34 ± 0.10	7	-7.1
29			H	9.00 ± 0.22	7	8.24 ± 0.10	7	-5.8
30			H	6.27 ± 0.20	4	6.71 ± 0.30	4	+2.8
31			H	7.06 ± 0.07	2	6.77 ± 0.39	2	-2.0
32			H	6.89 ± 0.12	4	7.12 ± 0.13	4	+1.7
10		NH ₂	H	8.53 ± 0.11	5	7.51 ± 0.32	5	-11
26		Me	H	8.59 ± 0.19	5	8.42 ± 0.09	5	-1.5
6		Et	H	9.20 ± 0.12	5	8.84 ± 0.46	8	-2.3
27		CF ₃	H	7.35 ± 0.15	3	7.42 ± 0.39	3	+1.2
14		Br	H	9.31 ± 0.16	6	8.85 ± 0.16	7	-2.9
VUF10166		Cl	H	9.82 ± 0.26	7	7.90 ± 0.49	6	-83
16		Cl	H	9.11 ± 0.26	3	8.34 ± 0.23	3	-5.9
18		Cl	H	6.69 ± 0.16	3	6.67 ± 0.02	3	-1.0
23		Cl	6-Cl	8.95 ± 0.18	7	7.85 ± 0.08	14	-13
11		Cl	6,7-Cl	8.09 ± 0.34	6	7.48 ± 0.16	6	-4.1

Table 1. (Continued)

Compd	R ¹	R ²	R ³		n	pK _i (AB)	n	Fold diff. ^[a]
			Chemical Structure	pK _i (A)				
22		OH	7-Cl	7.50 ± 0.13	3	8.14 ± 0.21	3	+4.3
34		OH	6,7-Cl	7.30 ± 0.39	6	7.14 ± 0.26	9	-1.4
24		H	H	8.21 ± 0.26	5	9.13 ± 0.30	5	+8.3
33		H	6-Cl	7.79 ± 0.20	3	6.99 ± 0.31	3	-6.3
7		H	6,7-Cl	8.41 ± 0.29	6	8.07 ± 0.27	5	-2.2
19		H	H	8.09 ± 0.20	5	7.48 ± 0.13	5	-4.0
21		H	H	7.49 ± 0.08	6	7.11 ± 0.15	5	-2.4

[a] +/- refer to an increase or decrease at 5-HT₃AB relative to 5-HT₃A.

seems that the tautomeric form in which the aromatic nitrogen atom represents a hydrogen bond donor is not involved in binding, as the conversion of the R² alcohol functionality of **1** into a methoxy (compound **28**) or ethoxy (compound **29**) group results in compounds with comparable affinities. However, larger ether analogues are not favorable for binding, as observed for compounds **30–32** in which the cyclohexyl, phenyl, and benzyl ether derivatives have ~100-fold lower affinities. When the hydroxy group of **1** at R² was changed to a different polar moiety (e.g., an amine moiety, as in compound **10**), the high affinity was maintained. A decreased affinity was observed for compound **26**, which incorporates a methyl group (which is electron-donating) at the R² position, relative to VUF10166. Addition of an electron-withdrawing CF₃ group (compound **27**) results in an even larger decrease in 5-HT₃A receptor affinity. Compounds that have chlorine or bromine atoms at this position have sub-nanomolar affinities (VUF10166 and **14**), indicating that the SAR in this position is very subtle, and an interplay between inductive and resonance effects cannot be ruled out.

For R²=Cl (VUF10166), different basic moieties were introduced. A small drop in affinity results from replacing R¹=N-methylpiperazine (VUF10166) with R¹=N-methylhomopiperazine (**16**), but a ~1000-fold drop in affinity is observed for R¹=N-methylpyrrolidin-3-amine (**18**). As the methylpiperazine moiety leads to the most potent compounds at 5-HT₃A receptors, this basic group was used in the R¹ position when exploring the effects of different chlorine substitution patterns at the R³ position. Addition of a 6-Cl at R² (compound **23**) causes a ~10-fold drop in affinity, and a second chlorine atom at posi-

tion R³ (6,7-Cl, **11**) results in another ~10-fold decrease. Again, VUF10166 (R³=H) shows the highest affinity for the 5-HT₃A receptor. For compounds with R²=OH (**1**), a similar trend is observed. Affinity at the 5-HT₃A receptor is highest for R³=H (**1**) and decreases significantly for both compound **22** (R³=6-Cl) and **34** (R³=6,7-Cl), which both have a pK_i in the mid-nanomolar range.

The same modifications to R¹ and R³ were made for the most simple 2-N-methylpiperazine quinoxaline compound of the series (R²=H, **24**), which has a pK_i of 8.21. Addition of chlorine atoms at position R³ (**33**, **7**) results in compounds with similar affinity at the 5-HT₃A receptor. Finally, replacement of the N-methylpiperazine group of compound **24** with an N-methylhomopiperazine group (**19**) has no effect on 5-HT₃A receptor affinity, but for R¹=N-methylpyrrolidin-3-amine (**21**), a small decrease in affinity is observed. This is different to what is observed for R²=Cl, where basic moieties other than the N-methylpiperazine group resulted in more pronounced differences in affinity (e.g., compare **19** and **21** with **16** and **18**, respectively).

Affinity differences at 5-HT₃A and 5-HT₃AB receptors

The affinity of compound **1** is slightly higher (2.7-fold) for 5-HT₃AB receptors than for 5-HT₃A receptors. Methoxy and ethoxy analogues **28** and **29** both show a 10-fold decrease in affinity at 5-HT₃AB receptors relative to compound **1**; in contrast, these modifications do not result in a change in affinity at the 5-HT₃A receptor. The larger ether analogues **30–32** have pK_i values of ~7 for the 5-HT₃AB receptor, which are similar to

their affinities for the homomeric receptor. Replacement of the alcohol moiety with an amine moiety (compound **10**) resulted in a large decrease in affinity (~70-fold) for 5-HT₃AB receptors but had little effect on the affinity for 5-HT₃A receptors. Similar affinities are observed at both the 5-HT₃A and 5-HT₃AB receptors for compounds that have methyl and ethyl substituents in the R² position (i.e., **26** and **6**, respectively), as well as for trifluoromethyl derivative **27**. For the halogen-substituted compounds, a different trend is observed. For R²=Br, the pK_i for 5-HT₃AB receptors is close to 9, which is similar to that for 5-HT₃A receptors, but the affinity of VUF10166 (R²=Cl) is significantly decreased at 5-HT₃AB receptors, resulting in a ~100-fold difference relative to 5-HT₃A receptors. The effect of replacing R¹=*N*-methylpiperazine (VUF10166) for R¹=*N*-methylhomopiperazine while R²=Cl (**16**) is negligible at 5-HT₃AB receptors, which is again different to what is observed at 5-HT₃A receptors. For R¹=*N*-methylpyrrolidin-3-amine (**18**), a >10-fold decrease in affinity for 5-HT₃AB receptors is observed. 5-HT₃AB receptor affinities for compounds with a chlorine atom at position R² (VUF10166, **23**, and **11**) do not change substantially when increasing numbers of chlorine atoms are added at the R³ position, although compound **11** has the lowest 5-HT₃AB receptor affinity of this subset. This is different to what is observed for the 5-HT₃A receptor affinities of these compounds, where addition of chlorine at R³ resulted in a large decrease in affinity. When R²=OH, compound **1** (R³=H) had the highest 5-HT₃AB receptor affinity, compound **22** (R³=6-Cl) showed a ~10-fold decrease in affinity, and a further ~10-fold decrease in affinity was observed for compound **34** (R³=6,7-Cl). 5-HT₃A receptor affinities shown by **22** and **34** are similar. When R²=H, the highest 5-HT₃AB receptor affinity was observed for R³=H (**24**), but a ~100-fold drop in affinity was observed for R³=6-Cl (**33**) and only a ~10-fold drop for R³=6,7-Cl (**7**). The effect on 5-HT₃AB receptor affinity when replacing R¹=*N*-methylpiperazine (**24**) for R¹=*N*-methylhomopiperazine (**19**), while R²=H, is a ~45-fold decrease in affinity. For compound **21**, a similar lowering in 5-HT₃AB receptor affinity is observed. This is in contrast to what is observed for 5-HT₃A receptors and can primarily be attributed to the sub-nanomolar affinity of compound **24** at 5-HT₃AB receptors, which is almost 10-fold higher than its 5-HT₃A receptor affinity.

Table 1 shows that compound **24** shows the highest selectivity for 5-HT₃AB over 5-HT₃A receptors (~10-fold), and VUF 10166 has the highest selectivity for 5-HT₃A over 5-HT₃AB receptors (~100-fold). The difference between these two compounds is solely the atom at position R², R²=H for compound **24** and R²=Cl for VUF10166. When the hydrogen atom is replaced with a chlorine atom, the 5-HT₃A receptor affinity increases ~40-fold, while the affinity for 5-HT₃AB receptors decreases ~20-fold. Both of these compounds comprise the *N*-methylpiperazine moiety, which is the preferred basic group for selectivity. For 5-HT₃A receptor affinity, R²=Cl (VUF10166) is superior, with Br (**14**), Et (**6**), OMe (**28**), and OEt (**29**) having similar lower affinities. For the 5-HT₃AB receptor, an alcohol moiety at position R² (as observed for compound **1**) is preferred, but a hydrogen atom at R² also results in high affinity (compound **24**). At 5-HT₃AB receptors, R²=Br and the smaller

alkyl (**26**, **6**) and ether analogues (**28** and **29**) also have high affinities, whereas incorporation of larger ether groups at R² results in decreased affinity. However, for R²=Cl (VUF10166) and NH₂ (**10**), only 5-HT₃AB receptor affinity is decreased, resulting in 100- and 10-fold selectivity for 5-HT₃A over 5-HT₃AB receptors, respectively. Different substitution patterns at the R³ position also caused marked changes. For example, when R²=Cl, replacement of R³=H (VUF10166) with a chlorine atom results in a ~10-fold (R³=6-Cl, **23**) or ~100-fold (R³=6,7-Cl, **11**) decrease in affinity for the 5-HT₃A receptor, but this replacement does not have a large effect on 5-HT₃AB receptor affinity. When R²=H, the affinity for 5-HT₃A receptors does not show a large difference upon addition of chlorine atoms to the R³ position, but the 5-HT₃AB receptor affinity changes significantly. It can be concluded that, in either case, the greatest 5-HT₃ receptor subtype selectivity is achieved for R¹=*N*-methylpiperazine.

5-HT₃ receptor binding sites

Orthosteric binding sites in 5-HT₃AB receptors could theoretically exist at A+A-, A+B-, B+A-, and B+B- interfaces, but the majority of 5-HT₃ receptor-competitive ligands only bind to an A+A- interface.^[4,10] There is evidence, however, that at least one of the quinoxaline compounds studied here (VUF10166) binds to both an A+A- and an A+B- interface; binding to the A+B- interface may decrease the affinity of ligands binding to the A+A- site by allosterically increasing the rate of ligand dissociation.^[7] Other quinoxalines may similarly bind to both sites; thus, to identify potential interactions, we constructed models of the two interfaces.

Homology models were based on a tropisetron-bound AChBP crystal structure (PDB code: 2WNC) as no quinoxaline-bound Cys-loop receptor structure has been solved to date, and tropisetron is the closest structurally related compound to those described here (Figure 3). Tropisetron is an antagonist at the 5-HT₃ receptor but can act as an agonist at some nACh receptors,^[11] thus, it is an ideal choice from the available structures as quinoxalines can act as both agonists and antagonists at 5-HT₃ receptors, though they were not evaluated in this study. As with all homology models, caution must be applied in data interpretation, especially now that recent electron microscope images of the nACh receptor have shown that the difference between the structure of unbound and agonist-bound binding site sites is less than that observed in AChBP.^[12] Nevertheless, it is likely that our compounds adopt a broadly similar orientation to tropisetron; therefore, the models serve as means of identifying residues that could potentially be responsible for the differences in affinities of the quinoxaline ligands at 5-HT₃A and 5-HT₃AB receptors. As discussed below, several of the identified residues are known to interact with a range of 5-HT₃ receptor ligands (Figures 2 and 3).^[4] Some of these are the same in both A+A- and A+B- binding sites and are unlikely to be responsible for differences in affinity, while others are different and may provide possible explanations for the varied ligand affinities at the two receptor subtypes.

consistent with all other 5-HT₃ receptor-competitive ligands.^[10,16] Some, however, show significant differences and thus may bind to the A + B⁻ interface as has previously been shown for VUF10166.^[10] These novel ligands could be valuable in both experimental and computer-aided drug design, with potential for the development of novel therapeutic agents.

Experimental Section

Chemistry: Chemicals and solvents were purchased from Sigma-Aldrich and used as received. Unless indicated otherwise, all reactions were carried out under an inert atmosphere of dry N₂. TLC analyses were performed with Merck F254 alumina silica plates using UV visualization or staining. Column purifications were carried out automatically using the Biotage equipment. All HRMS spectra were recorded on Bruker microTOF mass spectrometer using ESI in positive ion mode. ¹H NMR spectra were recorded on a Bruker 250 (250 MHz) or a Bruker 500 (500 MHz) spectrometer. Data are reported as follows: chemical shift, integration, multiplicity (s=singlet, d=doublet, t=triplet, br=broad, m=multiplet), and coupling constants (Hz). Chemical shifts are reported in ppm with the natural abundance of deuterium in the solvent as the internal reference (CHCl₃ in CDCl₃: δ=7.26 ppm and CH₃OH in CH₃OD: δ=3.31 ppm, (CD₃)₂SO in (CD₃)₂SO: δ=2.50 ppm). ¹³C NMR spectra were recorded on a Bruker 500 (126 MHz) spectrometer with complete proton decoupling. Chemical shifts are reported in ppm with the solvent resonance resulting from incomplete deuteration as the internal reference (CDCl₃: δ=77.16 ppm, CH₃OD: δ=49.00 ppm, (CD₃)₂SO: δ=39.52 ppm). Systematic names for molecules according to IUPAC rules were generated using the ChemDraw AutoNom program. Purity was determined using a Shimadzu HPLC/MS workstation with a LC-20AD pump system, SPD-M20A diode array detection, and an LCMS-2010 EV mass spectrometer. An Xbridge C₁₈ 5 μm column (100 mm × 4.6 mm) was used. Compound purities were calculated as the percentage peak area of the analyzed compound by UV detection at 230 nm. Solvents used were as follows: solvent B=CH₃CN 0.1% formic acid; solvent A=H₂O 0.1%. The analysis was conducted using a flow rate of 1.0 mL min⁻¹, starting at 5% B with a linear gradient to 90% B in 4.5 min, then 1.5 min at 90% B with a linear gradient to 5% B in 0.5 min, and then 1.5 min at 5% B, with a total run time of 8 min. Compounds **24–34** were synthesized by our group as described by Smits et al.^[9]

3-Ethyl-3,4-dihydroquinoxalin-2(1H)-one (4): Benzene-1,2-diamine (**2**) (1.07 g, 28.4 mmol) and 2-oxobutanoic acid (2.90 g, 28.4 mmol) were dissolved in 50 mL CH₃OH, and the resulting solution was stirred overnight at room temperature. The resulting precipitate was collected via filtration over a Büchner funnel. The precipitate was washed with cold CH₃OH and dried in a vacuum oven to yield 2.25 g (12.9 mmol, 46%) of **4** as an off-white solid: ¹H NMR (500 MHz, CDCl₃) δ=11.25 (s, 1H), 7.84 (d, J=8.1 Hz, 1H), 7.52–7.45 (m, 1H), 7.36–7.31 (m, 1H), 7.28 (d, J=7.8 Hz, 1H), 3.01 (q, J=7.4 Hz, 2H), 1.38 ppm (t, J=7.4 Hz, 3H); ¹³C NMR (126 MHz, CDCl₃) δ=162.54, 156.24, 132.91, 130.97, 129.57, 128.85, 124.09, 115.31, 26.85, 10.85 ppm.

6,7-Dichloro-3,4-dihydroquinoxalin-2(1H)-one (5): 4,5-dichlorobenzene-1,2-diamine (**3**) (842 mg, 4.76 mmol) and 2-oxoacetic acid (715 mg, 4.83 mmol) were dissolved in CH₃OH (50 mL) and stirred at room temperature for 30 min. The mixture was concentrated under reduced pressure, H₂O was added, and the resulting mixture was extracted with EtOAc. The combined organic phases were

dried over MgSO₄ and concentrated under reduced pressure to yield 133 mg of **5** (0.62 mmol, 13%) as a dark-brown solid: ¹H NMR (250 MHz, DMSO) δ=8.19 (s, 1H), 8.04 (s, 1H), 7.45 ppm (s, 1H).

2-Ethyl-3-(4-methylpiperazin-1-yl)quinoxaline (6): A solution of **4** (1.64 g, 9.39 mmol) in phosphoryl trichloride (100 mL) was stirred at 100 °C for 1 h. The reaction mixture was then concentrated under reduced pressure. H₂O was added to the remaining solid, then the mixture was extracted with CH₂Cl₂. The organic layers were combined, dried over Na₂SO₄, and concentrated under reduced pressure to yield 1.59 g (8.24 mmol, 88%) of 2-chloro-3-ethylquinoxaline as a dark-pink solid: ¹H NMR (250 MHz, CDCl₃) δ=8.10–8.03 (m, 1H), 8.02–7.95 (m, 1H), 7.79–7.67 (m, 2H), 3.17 (q, J=7.5 Hz, 2H), 1.44 ppm (t, J=7.5 Hz, 3H). Next, 2-chloro-3-ethylquinoxaline (555 mg, 2.88 mmol) was dissolved in *N*-methylpiperazine (2 mL), and the resulting solution was heated at 120 °C for 15 min using microwave (mw) radiation. After cooling to room temperature, excess *N*-methylpiperazine was removed under reduced pressure, and the product was purified over SiO₂ (EtOAc/Et₃N, 96:4, v/v) to yield 566 mg of **6** (2.21 mmol, 77%) as a yellow solid: ¹H NMR (250 MHz, CDCl₃) δ=7.95–7.87 (m, 1H), 7.85–7.78 (m, 1H), 7.61–7.45 (m, 2H), 3.43–3.31 (m, 4H), 2.97 (q, J=7.4 Hz, 2H), 2.68–2.58 (m, 4H), 2.38 (s, 3H), 1.41 ppm (t, J=7.4 Hz, 3H); ¹³C NMR (126 MHz, CDCl₃) δ=155.74, 154.15, 139.92, 138.88, 128.68, 128.01, 127.27, 126.57, 55.04, 49.67, 46.24, 27.70, 12.64 ppm; LCMS: t_R=2.82 min, purity 95%, [M+H]⁺ 257.00; HRMS *m/z*: [M+H]⁺ calcd for C₁₅H₂₁N₄: 257.1761, found: 257.1763.

6,7-Dichloro-2-(4-methylpiperazin-1-yl)quinoxaline (7): A solution of **5** (133 mg, 0.62 mmol) in phosphoryl trichloride (50 mL) was stirred at 100 °C for 1 h. The reaction mixture was concentrated under reduced pressure, H₂O was added to the remaining solid this, and the mixture was extracted with CH₂Cl₂. The organic layers were combined, dried over Na₂SO₄, and concentrated under reduced pressure to yield 66 mg (0.28 mmol, 46%) of 2,6,7-trichloroquinoxaline: ¹H NMR (250 MHz, CDCl₃) δ=8.77 (s, 1H), 8.25 (s, 1H), 8.15 ppm (s, 1H). Then, 2,6,7-trichloroquinoxaline (66 mg, 0.28 mmol) was dissolved in EtOAc (2 mL), *N*-methylpiperazine (0.1 mL, 0.90 mmol) was added, and the resulting solution was heated at 160 °C for 1 h using microwave radiation. After cooling to room temperature, EtOAc and excess *N*-methylpiperazine were removed under reduced pressure, and the product was purified over SiO₂ (EtOAc/Et₃N, 96:4, v/v) to yield 36 mg of **7** (0.12 mmol, 43%) as a light-brown solid: ¹H NMR (250 MHz, CDCl₃) δ=8.55 (s, 1H), 7.96 (s, 1H), 7.77 (s, 1H), 3.85–3.79 (m, 4H), 2.59–2.52 (m, 4H), 2.37 ppm (s, 3H); ¹³C NMR (126 MHz, CDCl₃) δ=152.87, 142.50, 139.15, 136.67, 134.50, 131.10, 128.26, 127.62, 54.60, 48.80, 46.07 ppm; LCMS: t_R=3.39 min, purity >99%, [M+H]⁺ 296.90; HRMS *m/z*: [M+H]⁺ calcd for C₁₃H₁₅Cl₂N₄: 297.0668, found: 297.0662.

3-(4-Methylpiperazin-1-yl)quinoxalin-2-amine (10): 2,3-Dichloroquinoxaline (**8**) (1.99 g, 10.0 mmol) was dissolved in a 2 M NH₃ solution in EtOH (5.5 mL) and heated in the microwave at 100 °C for 2 h. The solvent was then removed under reduced pressure, and the residue was purified over SiO₂ (CH₂Cl₂/EtOAc, 100:0 to 60:40, v/v) to give 300 mg (1.67 mmol, 17%) of 3-chloroquinoxalin-2-amine. Next, 3-chloroquinoxalin-2-amine (150 mg, 0.84 mmol) and *N*-methylpiperazine (1.0 mL, 9.02 mmol) were dissolved in THF (4 mL). The resulting mixture was heated under microwave conditions at 150 °C for 40 min, quenched with H₂O, and extracted with EtOAc. The organic layers were combined, dried (Na₂SO₄), and concentrated under reduced pressure. The product was crystallized from EtOAc to give 100 mg (0.41 mmol, 49%) of **10** as a dark-yellow solid: ¹H NMR (250 MHz, CDCl₃) δ=7.76 (d, J=7.8 Hz, 1H),

7.60 (d, $J=7.8$ Hz, 1H), 7.50–7.33 (m, 2H), 4.98 (s, 2H), 3.56–3.27 (m, 4H), 2.76–2.51 (m, 4H), 2.46–2.29 ppm (m, 3H); ^{13}C NMR (126 MHz, CDCl_3) $\delta=148.39, 147.69, 138.94, 137.41, 127.34, 127.26, 125.25, 125.08, 55.07, 48.54, 46.24$ ppm; LCMS: $t_{\text{R}}=2.25$ min, purity $>99\%$, $[M+H]^+$ 244.00; HRMS m/z : $[M+H]^+$ calcd for $\text{C}_{13}\text{H}_{18}\text{N}_5$: 244.1557, found: 224.1552.

2,6,7-Trichloro-3-(4-methylpiperazin-1-yl)quinoxaline (11): 2,3,6,7-Tetrachloroquinoxaline (**9**) (1.23 g, 4.58 mmol) was dissolved in THF (50 mL). *N*-methylpiperazine (0.58 mL, 4.58 mmol) and triethylamine (0.65 mL, 4.66 mmol) were added, and the mixture was stirred at 80 °C for 96 h, quenched with H_2O , and extracted with EtOAc. The organic layers were combined, dried over MgSO_4 , and concentrated under reduced pressure to yield 1.02 g (3.08 mmol, 67%) of **11** as a light-brown solid: ^1H NMR (250 MHz, CDCl_3) $\delta=7.95$ (s, 1H), 7.92 (s, 1H), 3.68–3.59 (m, 4H), 2.66–2.58 (m, 4H), 2.38 ppm (s, 3H); ^{13}C NMR (126 MHz, CDCl_3) $\delta=152.87, 142.50, 139.15, 136.67, 134.50, 131.10, 128.26, 127.62, 54.60, 48.80, 46.07$ ppm; LCMS: $t_{\text{R}}=3.64$ min, purity $>99\%$, $[M+H]^+$ 330.85; HRMS m/z : $[M+H]^+$ calcd for $\text{C}_{13}\text{H}_{14}\text{Cl}_3\text{N}_4$: 331.0279, found: 331.0271.

2,3-Dibromoquinoxaline (13): Quinoxaline-2,3-diol (**12**) (2.96 g, 18.3 mmol) and pentabromophosphorane (17.06 g, 39.6 mmol) were suspended in toluene (200 mL) and heated at 160 °C for 3 h. After cooling to room temperature, ice water (200 mL) was added to the solution, and the mixture was stirred vigorously for 30 min. The mixture was extracted with toluene, washed with 1 *N* NaOH (100 mL), dried over MgSO_4 , filtered, and concentrated under vacuum. The crude product was purified over SiO_2 ($\text{CH}_2\text{Cl}_2/n$ -heptanes, 1:2, *v/v*) to give 505 mg (12.7 mmol, 70%) of **13** as a beige solid: ^1H NMR (250 MHz, CDCl_3) $\delta=8.09$ –8.00 (m, 2H), 7.86–7.77 ppm (m, 2H).

2-Bromo-3-(4-methylpiperazin-1-yl)quinoxaline (14): 2,3-Dibromoquinoxaline (**13**) (505 mg, 1.75 mmol), *N*-methylpiperazine (176 mg, 1.75 mmol), and Et_3N (177 mg, 1.75 mmol) were dissolved in toluene (50 mL). The solution was stirred at 160 °C for 6 h. After cooling to room temperature, H_2O was added, and the emulsion was extracted with toluene. The combined organic extracts were dried over MgSO_4 and concentrated under vacuum. The crude product was purified over SiO_2 (EtOAc/ Et_3N , 98:2, *v/v*) to give 377 mg (1.23 mmol, 70%) of **14** as a beige solid: ^1H NMR (250 MHz, CDCl_3) $\delta=7.90$ (dd, $J=8.3, 1.2$ Hz, 1H), 7.83 (dd, $J=8.3, 1.1$ Hz, 1H), 7.70–7.61 (m, 1H), 7.58–7.48 (m, 1H), 3.63–3.55 (m, 4H), 2.69–2.61 (m, 4H), 2.39 ppm (s, 3H); ^{13}C NMR (126 MHz, CDCl_3) $\delta=153.60, 140.03, 139.18, 134.98, 130.25, 127.86, 127.40, 127.19, 54.70, 49.48, 46.18$ ppm; LCMS: $t_{\text{R}}=2.69$ min, purity $>99\%$, $[M+H]^+$ 306.90; HRMS m/z : $[M+H]^+$ calcd for $\text{C}_{13}\text{H}_{16}\text{BrN}_4$: 307.0553, found: 307.0552.

2-Chloro-3-(4-methyl-1,4-diazepan-1-yl)quinoxaline (16): 2,3-Dichloroquinoxaline (**8**) (1.00 g, 5.0 mmol), *N*-methyl-1,4-diazepane (0.86 mL, 7.50 mmol), and Et_3N (0.70 mL, 5.00 mmol) were dissolved in toluene (50 mL). The solution was stirred overnight at reflux. After cooling to room temperature, H_2O was added, and the resulting mixture was extracted with toluene, dried over MgSO_4 , and concentrated under vacuum. The crude was purified over SiO_2 (EtOAc/ Et_3N , 99:1, *v/v*) to give 1.01 g (3.65 mmol, 73%) of **16** as a yellow oil: ^1H NMR (500 MHz, CDCl_3) $\delta=7.87$ –7.76 (m, 1H), 7.76–7.69 (m, 1H), 7.58 (ddd, $J=8.4, 7.0, 1.4$ Hz, 1H), 7.44 (ddd, $J=8.3, 7.0, 1.4$ Hz, 1H), 3.90–3.86 (m, 2H), 3.86–3.81 (m, 2H), 2.90–2.83 (m, 2H), 2.70–2.64 (m, 2H), 2.42 (s, 3H), 2.10 ppm (dt, $J=7.0, 6.0$ Hz, 2H); ^{13}C NMR (126 MHz, CDCl_3) $\delta=151.91, 140.04, 139.18, 137.27, 130.04, 127.52, 126.40, 126.04, 58.57, 57.51, 50.61, 50.33, 46.93,$

28.06 ppm; LCMS: $t_{\text{R}}=2.89$ min, purity $>99\%$, $[M+H]^+$ 277.10; HRMS m/z : $[M+H]^+$ calcd for $\text{C}_{14}\text{H}_{18}\text{ClN}_4$: 277.1215, found: 277.1210.

tert-Butyl (1-(3-chloroquinoxalin-2-yl)pyrrolidin-3-yl)(methyl)carbamate (17): 2,3-dichloroquinoxaline (0.54 g, 2.71 mmol) was dissolved in DMF (30 mL). K_2CO_3 (0.37 g, 2.71 mmol) and *tert*-butyl methyl(pyrrolidin-3-yl)carbamate (0.49 g, 2.47 mmol) were added, and the mixture was stirred at 90 °C for 4 h. The mixture was cooled to room temperature, diluted with H_2O , and extracted with Et_2O . The combined organic layers were dried over MgSO_4 and concentrated under reduced pressure to give 0.68 g of **17**, which was directly used in the synthesis of **18**.

1-(3-Chloroquinoxalin-2-yl)-*N*-methylpyrrolidin-3-amine (18): Compound **17** (0.40 g) was dissolved in dioxane (10 mL) and stirred at room temperature. A 4 *M* solution of HCl in dioxane (20 mL) was added dropwise, and precipitation was observed. The resulting suspension was stirred overnight and subsequently filtered over a Büchner funnel, and the residue was washed with 1,4-dioxane. The residue was then dried under reduced pressure to yield 202 mg of **18** as a light-yellow solid (0.68 mmol, 61%): ^1H NMR (500 MHz, CDCl_3) $\delta=7.87$ –7.74 (m, 2H), 7.68 (ddd, $J=8.4, 7.1, 1.4$ Hz, 1H), 7.58–7.46 (m, 1H), 4.27–4.10 (m, 3H), 4.10–3.92 (m, 2H), 2.83 (s, 3H), 2.61–2.45 (m, 1H), 2.37–2.23 ppm (m, 1H); ^{13}C NMR (126 MHz, CDCl_3) $\delta=147.42, 137.60, 136.72, 136.02, 131.08, 127.39, 126.50, 123.29, 57.92, 52.40, 48.69, 31.08, 27.60$ ppm; LCMS: $t_{\text{R}}=2.90$ min, purity 99%, $[M+H]^+$ 263.05; HRMS m/z : $[M+H]^+$ calcd for $\text{C}_{13}\text{H}_{16}\text{ClN}_4$: 263.1058, found: 263.1055.

2-(4-Methyl-1,4-diazepan-1-yl)quinoxaline (19): 2-Chloroquinoxaline (**15**) (2.97 g, 18.0 mmol), *N*-methyl-1,4-diazepane (3.3 mL, 24.0 mmol), and Et_3N (2.5 mL, 18.0 mmol) were dissolved in toluene (50 mL). The solution was stirred overnight at reflux. After cooling to room temperature, H_2O was added, and the resulting mixture was extracted with toluene, dried over MgSO_4 , and concentrated under vacuum. The crude residue was purified over SiO_2 (EtOAc/ Et_3N , 98:2, *v/v*) to give 3.12 g (12.9 mmol, 71%) of **19** as an off-white solid: ^1H NMR (250 MHz, CDCl_3) $\delta=8.47$ (s, 1H), 7.86 (d, $J=8.2$ Hz, 1H), 7.65 (d, $J=8.4$ Hz, 1H), 7.59–7.49 (m, 1H), 7.39–7.29 (m, 1H), 4.02–3.93 (m, 2H), 3.86 (t, $J=6.3$ Hz, 2H), 2.77 (dd, $J=5.7, 4.2$ Hz, 2H), 2.65–2.53 (m, 2H), 2.39 (s, 3H), 2.15–2.00 ppm (m, 2H); ^{13}C NMR (126 MHz, CDCl_3) $\delta=151.59, 142.03, 136.46, 134.92, 129.96, 128.65, 126.33, 123.98, 58.18, 57.25, 46.73, 46.55, 46.24, 27.48$ ppm; LCMS: $t_{\text{R}}=2.40$ min, purity $>99\%$, $[M+H]^+$ 243.00; HRMS m/z : $[M+H]^+$ calcd for $\text{C}_{14}\text{H}_{19}\text{N}_4$: 243.1604, found: 243.1608.

tert-Butyl methyl(1-(quinoxalin-2-yl)pyrrolidin-3-yl)carbamate (20): 2-Chloroquinoxaline (1.79 g, 10.9 mmol) was dissolved in DMF (50 mL). K_2CO_3 (1.51 g, 10.9 mmol) and *tert*-butyl methyl(pyrrolidin-3-yl)carbamate (2.00 g, 10.0 mmol) were added, and the mixture was stirred at 90 °C for 6 h. The mixture was cooled to room temperature, diluted with H_2O , and extracted with Et_2O . The combined organic layers were dried over MgSO_4 and concentrated under reduced pressure to give 3.28 g of **20**, which was directly used in the synthesis of **21**.

***N*-Methyl-1-(quinoxalin-2-yl)pyrrolidin-3-amine (21):** Compound **20** (2.95 g) was dissolved in dioxane (20 mL) and stirred at room temperature. A solution of 4 *M* HCl in dioxane (10 mL) was added dropwise, and precipitation was observed. The suspension was stirred overnight and filtered over a Büchner funnel. The residue was washed with 1,4-dioxane and dried under vacuum to yield 1.33 g of **21** as a beige solid (5.02 mmol, 56%): ^1H NMR (500 MHz, DMSO) $\delta=9.69$ –9.52 (m, 2H), 8.58 (s, 1H), 7.89–7.82 (m, 1H), 7.72

(d, $J=8.2$ Hz, 1H), 7.67–7.58 (m, 1H), 7.45–7.37 (m, 1H), 4.00–3.85 (m, 4H), 3.78–3.69 (m, 1H), 2.65–2.58 (m, 3H), 2.46–2.29 ppm (m, 2H); ^{13}C NMR (126 MHz, DMSO) $\delta=149.63, 140.28, 138.07, 136.38, 130.79, 129.12, 125.36, 124.68, 57.49, 49.25, 45.20, 31.42, 27.86$ ppm; LCMS: $t_{\text{R}}=2.41$ min, purity 97%, $[M+H]^+$ 229.10; HRMS m/z : $[M+H]^+$ calcd for $\text{C}_{13}\text{H}_{17}\text{N}_4$: 229.1448, found: 229.1454.

3,6-Dichloro-2-(4-methylpiperazin-1-yl)quinoxaline (23): DiPEA (0.38 mL, 2.15 mmol) and POCl_3 (2.00 mL, 21.5 mmol) were added to a solution of 7-chloro-3-(4-methylpiperazin-1-yl)quinoxalin-2(1H)-one (22) (300 mg, 1.08 mmol) in toluene (20 mL). The resulting mixture was stirred at reflux for 20 h, after which the mixture was concentrated under reduced pressure. H_2O (50 mL) and 1 M $\text{NaOH}_{(\text{aq})}$ (10 mL) were added to the crude product, and the resulting mixture was extracted with CH_2Cl_2 . The combined organic layers were washed with brine (50 mL), dried over NaSO_4 , and concentrated under reduced pressure. The crude product was purified over SiO_2 ($\text{EtOAc}/\text{Et}_3\text{N}$, 50:1, v/v) to give 270 mg of 23 (0.91 mmol, 84%) as a yellow solid: ^1H NMR (500 MHz, CDCl_3) $\delta=7.85$ (d, $J=2.3$ Hz, 1H), 7.75 (d, $J=8.9$ Hz, 1H), 7.57 (dd, $J=8.9, 2.3$ Hz, 1H), 3.69–3.54 (m, 4H), 2.72–2.56 (m, 4H), 2.38 ppm (s, 3H); ^{13}C NMR (126 MHz, CDCl_3) $\delta=152.58, 142.61, 138.75, 138.30, 132.59, 130.91, 128.14, 126.71, 54.70, 48.94, 46.15$ ppm; LCMS: $t_{\text{R}}=3.40$ min, purity < 99%, $[M+H]^+$ 196.90; HRMS m/z : $[M+H]^+$ calcd for $\text{C}_{13}\text{H}_{15}\text{Cl}_2\text{N}_4$: 297.0668, found: 297.0671.

Radioligand binding: This was carried out as previously described.^[6,7,10] Briefly, HEK293 cells expressing either 5-HT_{3A} or 5-HT_{3AB} receptors were scraped into 1 mL of ice-cold HEPES buffer (10 mM, pH 7.4) and frozen. After thawing, they were washed with HEPES buffer and homogenized using a fine-bore syringe. For competition binding experiments, 50 μL of cell membranes were incubated in 0.5 mL HEPES buffer containing a final concentration of 0.7 nM [^3H]granisetron ($\sim K_{\text{d}}$), both with and without the test compound. To ensure that there were no changes in the K_{d} of [^3H]granisetron, which could influence the K_{i} values of competing ligands, saturation binding curves were run in parallel with competition studies. Competition binding experiments using ten concentrations of ligands were performed on at least three separate plates of cells. Nonspecific binding was determined using 1 mM quipazine. Reactions were incubated for at least 24 h at 4 °C to allow compounds with slow kinetics to equilibrate. Experiments on 5-HT_{3A} and 5-HT_{3AB} receptors were run in parallel. Incubations were terminated by vacuum filtration using a Brandel cell harvester (Alpha Biotech Ltd., London, UK) onto GF/B filters pre-soaked in 0.3% polyethyleneimine. Radioactivity was determined by scintillation counting. Data were fit according to Equation (1):

$$B_L = B_{\text{min}} + \frac{B_{\text{max}} - B_{\text{min}}}{1 + 10^{\eta_{\text{H}}(\log L_{50} - \log L)}} \quad (1)$$

in which L is the concentration of ligand present, B_L is the binding in the presence of ligand concentration L , B_{min} is the binding when $L=0$, B_{max} is the binding when $L=\infty$, L_{50} is the concentration of L which gives a binding equal to $(B_{\text{max}} + B_{\text{min}})/2$, and η_{H} is the Hill coefficient. K_{i} values were estimated from IC_{50} values using the Cheng–Prusoff equation^[17] $K_{\text{i}} = \text{IC}_{50}/(1+[L]/K_{\text{d}})$, for which K_{i} is the equilibrium dissociation constant for binding of the unlabeled antagonist, IC_{50} is the concentration of antagonist that blocks half the specific binding, $[L]$ is the free concentration of radioligand, and K_{d} is the equilibrium dissociation constant of the radioligand.

Homology modeling: Construction of the homomeric 5-HT_{3A} receptor binding site model has been previously described.^[18] Using the same approach, a model of the 5-HT_{3AB} receptor binding site was

constructed by homology modeling using MOE (version 2010.10, Chemical Computing Group, Montreal). The sequence of the human 5-HT_{3AB} gene (O95264) was aligned with the sequence of the 5-HT_{3A} gene (P46098) using the “Protein Align” option in MOE (standard settings) and was adjusted manually. The final sequence alignment is shown in Figure 2. The 5-HT_{3A} receptor homology model was selected to serve as the template. Structural waters located in the binding pocket of the original crystal structure (PDB code: 2WNC)^[19] form a conserved protein–ligand hydrogen bond interaction network in several other AChBP crystals (e.g., 2BYR, 2PGZ, 2BYS, 2XYT) and were included in the 5-HT_{3AB} receptor model. The template backbone, the ligand, and the water molecules were fixed, and ten receptor models were constructed based on the template backbone. During this construction, the ligand and waters of the original co-crystal structure were considered as an additional restraint using the “Environment” option within MOE. The structural quality of the models was checked using the evaluation modules in MOE; protein geometry of receptor atoms was evaluated for bond lengths, bond angles, atom clashes, and contact energies. Ramachandran plots were used to check the Phi and Psi angles of all residues. The best model was selected for further refinement, hydrogen atoms were added, partial atomic charges were calculated, and the protein was minimized around the fixed ligand and static water molecules using the Amber99 force field in MOE.

Acknowledgements

This work was supported by a grant from the Wellcome Trust [081925] to S.C.R.L. and an EU FP7 grant (NeuroCypres) to I.d.E. and S.C.R.L.. S.C.R.L. is a Wellcome Trust Senior Research Fellow in Basic Biomedical Science. We thank Danny van Willigen and Linda Silvestri for excellent technical assistance.

Keywords: Cys loops • heteromers • homomers • 5-HT₃ receptors • quinoxalines • serotonin • subtypes

- [1] a) J. Walstab, G. Rappold, B. Niesle, *Pharmacol. Ther.* **2010**, *128*, 146–169; b) A. J. Thompson, S. C. Lummis, *Curr. Pharm. Des.* **2006**, *12*, 3615–3630; c) A. J. Thompson, S. C. Lummis, *Expert Opin. Ther. Targets* **2007**, *11*, 527–540.
- [2] a) X. Q. Hu, R. W. Peoples, *J. Biol. Chem.* **2008**, *283*, 6826–6831; b) B. Niesler, J. Kapeller, C. Hammer, G. Rappold, *Pharmacogenomics* **2008**, *9*, 501–504.
- [3] A. A. Jensen, P. A. Davies, H. Brauner-Osborne, K. Krzykowski, *Trends Pharmacol. Sci.* **2008**, *29*, 437–444.
- [4] A. J. Thompson, H. A. Lester, S. C. Lummis, *Q. Rev. Biophys.* **2010**, *43*, 449–499.
- [5] a) S. P. Kelley, J. I. Dunlop, E. F. Kirkness, J. J. Lambert, J. A. Peters, *Nature* **2003**, *424*, 321–324; b) A. E. Dubin, R. Huvar, M. R. D’Andrea, J. Pyati, J. Y. Zhu, K. C. Joy, S. J. Wilson, J. E. Galindo, C. A. Glass, L. Luo, M. R. Jackson, T. W. Lovenberg, M. G. Erlander, *J. Biol. Chem.* **1999**, *274*, 30799–810.
- [6] a) A. J. Thompson, R. K. Duke, S. C. Lummis, *Mol. Pharmacol.* **2011**, *80*, 183–190; b) P. Das, G. H. Dillon, *Brain Res. Mol. Brain Res.* **2003**, *119*, 207–12.
- [7] A. J. Thompson, M. H. P. Verheij, I. J. P. de Esch, S. C. R. Lummis, *J. Pharmacol. Exp. Ther.* **2012**, *341*, 350–359.
- [8] a) S. Butini, R. Budriesi, M. Hamon, E. Morelli, S. Gemma, M. Brindisi, G. Borrelli, E. Novellino, I. Fiorini, P. Ioan, A. Chiarini, A. Cagnotto, T. Mennini, C. Fracasso, S. Caccia, G. Campiani, *J. Med. Chem.* **2009**, *52*, 6946–6950; b) G. Campiani, A. Cappelli, V. Nacci, M. Anzini, S. Vomero, M. Hamon, A. Cagnotto, C. Fracasso, C. Ubaldi, S. Caccia, S. Consolo, T. Mennini, *J. Med. Chem.* **1997**, *40*, 3670–3678; c) R. Mahesh, R. V. Peru-

- mal, P. V. Pandi, *Bioorg. Med. Chem. Lett.* **2004**, *14*, 5179–5181; d) R. Mahesh, T. Devadoss, D. K. Pandey, S. Bhatt, S. K. Yadav, *Bioorg. Med. Chem. Lett.* **2010**, *20*, 6773–6776; e) A. Monge, J. A. Palop, J. C. Del Castillo, J. M. Caldero, J. Roca, G. Romero, J. Del Rio, B. Lasheras, *J. Med. Chem.* **1993**, *36*, 2745–2750.
- [9] R. A. Smits, H. D. Lim, A. Hanzer, O. P. Zuiderveld, E. Guaita, M. Adami, G. Coruzzi, R. Leurs, I. J. P. de Esch, *J. Med. Chem.* **2008**, *51*, 2457–2467.
- [10] A. J. Thompson, K. L. Price, S. C. R. Lummis, *J. Physiol.* **2011**, *589*, 4243–4257.
- [11] R. L. Papke, J. K. P. Papke, G. M. Rose, *Bioorg. Med. Chem. Lett.* **2004**, *14*, 1849–1853.
- [12] N. Unwin, Y. J. Fujiyoshi, *J. Mol. Biol.* **2012**, *422*, 617–34.
- [13] a) D. L. Beene, G. S. Brandt, W. Zhong, N. M. Zacharias, H. A. Lester, D. A. Dougherty, *Biochemistry* **2002**, *41*, 10262–10269; b) D. L. Beene, K. L. Price, H. A. Lester, D. A. Dougherty, S. C. Lummis, *J. Neurosci.* **2004**, *24*, 9097–9104; c) K. L. Price, S. C. Lummis, *J. Biol. Chem.* **2004**, *279*, 23294–23301; d) K. L. Price, K. S. Bower, A. J. Thompson, H. A. Lester, D. A. Dougherty, S. C. R. Lummis, *Biochemistry* **2008**, *47*, 6370–6377; e) A. J. Thompson, M. Lochner, S. C. Lummis, *Biophys. J.* **2008**, *95*, 5728–5736; f) A. J. Thompson, K. L. Price, D. C. Reeves, S. L. Chan, P. L. Chau, S. C. Lummis, *J. Biol. Chem.* **2005**, *280*, 20476–20482; g) P. Venkataraman, P. Joshi, S. P. Venkatachalan, M. Muthalagi, H. S. Parihar, K. S. Kirschbaum, M. K. Schulte, *BMC Biochem.* **2002**, *3*, 16; h) D. Yan, M. K. Schulte, K. E. Bloom, M. M. White, *J. Biol. Chem.* **1999**, *274*, 5537–5541.
- [14] a) A. Asagarasu, T. Matsui, H. Hayashi, S. Tamaoki, Y. Yamauchi, M. Sato, *Chem. Pharm. Bull.* **2009**, *57*, 34–42; b) A. Cappelli, M. Anzini, S. Vomero, L. Mennuni, F. Makovec, E. Doucet, M. Hamon, M. C. Menziani, P. G. De Benedetti, G. Giorgi, C. Ghelardini, S. Collina, *Bioorg. Med. Chem.* **2002**, *10*, 779–801; c) R. D. Clark, A. B. Miller, J. Berger, D. B. Repke, K. K. Weinhardt, B. A. Kowalczyk, R. M. Eglen, D. W. Bonhaus, C. H. Lee, *J. Med. Chem.* **1993**, *36*, 2645–2657; d) S. Evans, A. Galdes, M. Gall, *Pharmacol. Biochem. Behav.* **1991**, *40*, 1033–1040; e) M. Hibert, R. Hoffmann, R. Miller, A. Carr, *J. Med. Chem.* **1990**, *33*, 1594–1600; f) R. Mahesh, R. V. Perumal, P. V. Pandi, *Biol. Pharm. Bull.* **2004**, *27*, 1403–1405.
- [15] D. Yan, M. M. White, *Mol. Pharmacol.* **2005**, *68*, 365–371.
- [16] J. Peters, M. Cooper, M. Livesey, J. Carland, J. Lambert in *Ion Channels: From Structure to Function* (Eds.: J. N. C. Kew, C. H. Davies), Oxford University Press, **2010**, pp. 231–251.
- [17] Y. Cheng, W. H. Prusoff, *Biochem. Pharmacol.* **1973**, *22*, 3099–30108.
- [18] M. H. P. Verheij, A. J. Thompson, J. E. van Muijlwijk-Koezen, S. C. R. Lummis, R. Leurs, I. J. P. de Esch, *J. Med. Chem.* **2012**, *55*, 8603–14.
- [19] R. E. Hibbs, G. Sulzenbacher, J. Shi, T. T. Talley, S. Conrod, W. R. Kem, P. Taylor, P. Marchot, Y. Bourne, *EMBO J.* **2009**, *28*, 3040–3051.

Received: January 22, 2013

Revised: March 15, 2013

Published online on ■ ■ ■, 0000